U.R.S.I. FRANCE JS 20 FUTURE NETWORKS: 5G AND BEYOND

Numerical dosimetry in human model for 5G and beyond
Dosimétrie numérique dans le modèle humain pour la 5G et au-delà

Abdelrahman Ijjeh[1], Marylène Cueille[1], Jean-Lou Dubard[1], Michel Ney[2]
[1] LEAT, UMR-CNRS 7248, Université Côte d'Azur, 930 route des Colles, 06903 Sophia Antipolis, France
[2] Lab-STICC/IMT-Atlantique, CS 83818, 29238 Brest Cedex 3, France, michel.ney@imt-atlantique.fr

Keywords (in English and French):
SAR computation, sub-gridding, time-domain computational methods, complex media.
Calcul de DAS, sous-maillage, méthodes de calcul dans le domaine temporel, milieux complexes.

Abstract/Résumé

To design any new EM-device, it is of great importance to have a good estimation of the specific absorption rate (SAR) distribution or the Power Density (PD) it induces in users or people in its proximity. Respecting the recommended SAR limits is mandatory for any new technology to go public. Moreover, the good knowledge of SAR/PD is critical in any electromagnetic compatibility (EMC) study between EM-devices with lossy media. From numerical analysis point of view, as frequencies go higher and higher e.g. from 5G to millimetric or even terahertz applications, the computational problem becomes exhaustive in size. Note that at higher frequencies, the transmitting devices get normally smaller in size. In this article, we will study the effect of considering only the tissues (the part of the human model) adjacent to the transmitter vs. including the full human model in the computation domain. For a good spatial representation, the block-meshing scheme can be applied to finely mesh the antenna system and the tissues close to it. Numerical examples show the SAR distributions at 3.5 GHz in human head and the entire body, in addition to show the validity and CPU-time/memory gain obtained when considering part of the human model instead of the entire model. Moreover, we show the effects of human head presence on the antenna performance in its proximity.

1 Introduction

In the last few decades, one can observe the constant and rapid increase in operating frequencies of EM-devices. The reasons behind that is to increase the data rate (bandwidth), downsize antenna systems, and to allocate new unused frequency bands, in addition to other applications such as spectroscopy and imaging techniques. For such devices, the SAR/PD levels estimation is mandatory. However, at such high frequencies (5G and beyond) experimental measurements are very difficult to conduct [1] [2]. Even numerical simulations are very challenging in several scenarios [1] [2]. As the frequency goes higher the size of the computational domain becomes higher, hence the memory requirements and CPU time become higher as well. For instance at frequencies greater than 10 GHz, volumic simulations including human body are extremely huge and parallel big machines are necessary to perform the computations. It is worth mentioning that if we go the other way in the spectrum for instance to study the SAR at frequencies less than 10 MHz we face another problem; a huge number of iterations is necessary to cover the low frequency band of interest. Therefore, the easiest SAR computations with reasonable computational costs are for the range of frequencies between few tens of MHz until few GHz.

In this article, we are going to present a general methodology to perform SAR full-wave computations, as well as, focusing attention on the complexity of the problem, the different challenges and the practical computational limitations. Moreover, sub-gridding feature (it is much more efficient than structured irregular meshing that is used in the up-to-date commercial solvers) can be applied when dealing with a multi-scale scenario (ex. an antenna with very small details). Finally, we will study the effects of truncating the computational problem by keeping the antenna system and the human tissues in its proximity and excluding everything else.

2 Mathematical model

As a computational scheme, we are going to use the Transmission-Line Matrix method (TLM) in time-domain (TD). The TLM method is a full-wave computational method that has some very attractive features:

1) Can handle any linear anisotropic dispersive heterogeneous media [3].
2) Very efficient in highly heterogeneous structures (mesh or media), as compared to other TD methods.
3) One can do the sub-gridding for any mesh ratio, and in any heterogeneous media. Thanks to the ideal transformer model, that allows smooth, lossless and stable transition between fine and coarse meshes [4].

4) Can handle any lumped element (source, passive or active element). Thus, at any point (or region) we can define a port for example and control exactly how much power is supplied.

For more details concerning the mathematical representation of TLM method, we refer the reader to [3] [4].
As a human model, we used the heterogeneous Duke voxel model. Media properties for different tissues in are represented as a summation of four Cole-Cole expressions [5]:

$$\varepsilon(\omega) = \varepsilon_\infty + \sum_{i=1}^{4} \frac{\Delta\varepsilon_i}{(1+j\omega\tau_i)^{(1-\alpha_i)}} + \frac{\sigma}{j\omega\varepsilon_o} \quad (1)$$

where ε_∞ is the permittivity at very high frequencies, σ the conductivity, τ_i, $\alpha_i$and $\Delta\varepsilon_i$ are different parameters used by Cole-Cole model. In TD simulations, the dispersive media properties are translated into TD-filters.

3 SAR computation in realist scenarios

As frequencies go higher, the wavelength λ gets smaller. Finer meshes are required to represent the computational domain $\left(\Delta l \leq {}^{\lambda}/_{10\sqrt{\varepsilon_r}}\right)$. To show the complexity of the problem when working at higher frequencies we can make this rough estimation of the problem size. It is desired to simulate a human model exposed to a signal at 10 GHz ($\lambda = 3$ cm). Assuming the human model is mainly water ($\varepsilon_r \approx 70$) at 10 GHz and at 37 ºC, the mesh size is $dl \leq 0.36$ mm. Now for Duke model of dimensions 177 cm × 61 cm × 31 cm, one needs around 7.17 billion cells. To perform a convergence test for instance by doubling the resolution in every dimension, the problem size explodes to 57 billion of cells. For the 5G frequency band at 60 GHz the previous number of cells reaches few Tera cells. At millimetric (110 GHz to 300 GHz) and terahertz (0.3 THz to 30 THz) frequencies, cell numbers are much higher.

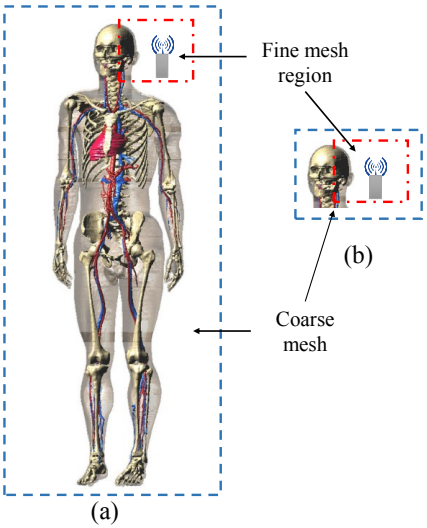

Figure 1: Duke model exposed to EM waves, (a) the full body is included in the computational domain, block meshing is used around the antenna system and the human tissues close to it. (b) Only the head is considered, fine resolution is used around the antenna and the tissues in its proximity.

As shown in figure 1, we are going to study the effect of considering only the part of Duke model that is close to the antenna system, for example the head in figure 1b. Comparison will be made with the scenario when the full body is present (figure 1a). The objective is to compute the impact of truncating the computational domain on the SAR distribution in human head and on the antenna performance. Such analysis can be very beneficial when dealing with devices that produces localized power in small regions such as medical sensors and RFIDs, smart lenses, or other wearable devices. Sub-gridding feature in TLM can used to give a good geometrical representation of the antenna system/circuit and the nearby human tissues. Finally, as frequencies go higher, the skin effect obliges us to use fine resolution in the first few skin depths in lossy media to accurately capture the rapidly decaying EM fields.

4 Results and discussions

In this section, we present three scenarios for SAR computation at 3.5 GHz frequency. In the first experiment, we study the effects of plane-wave excitation on the head of Duke voxel model for two spatial resolutions (mesh

sizes), namely, at $\Delta x = 1$ mm and at $\Delta x = 0.667$ mm. In the second experiment, the SAR distribution is shown when Duke' head is excited by a half-wavelength dipole antenna ($\lambda = 8.6$ cm) at the aforementioned resolutions. In addition, the impact of human head presence on the antenna input impedance is presented. Finally, an experiment of SAR computation again at 3.5 GHz is provided for plane wave excitation with both the head alone, and the entire body. The objective of this experiment is to show the effects of exclusion the rest of the body on the accuracy in SAR distributions in the head. To reduce the computer expenditures, we used a resolution of 2 mm for the last experiment, since the entire human model was very huge to simulate at 1 mm or finer. In all experiments cubic cells were used everywhere, with maximum time-step. Modulated-Gaussian pulse ($t_o = 6.67$ ns, $\sigma = 1.33$ ns and $f_o = 3.5$ GHz) was used as an excitation. All simulations were performed on a TLM parallel solver developed in collaboration between LEAT laboratory and IMT-Atlantique [6].

4.1 Duke' head excited by a plane wave

Consider the configuration in Figure 2 below with the head of Duke' model illuminated by a plane wave. Huygens box for is used as a source of plane wave excitation. The TEM wave is vertically polarized propagating towards the face of Duke.

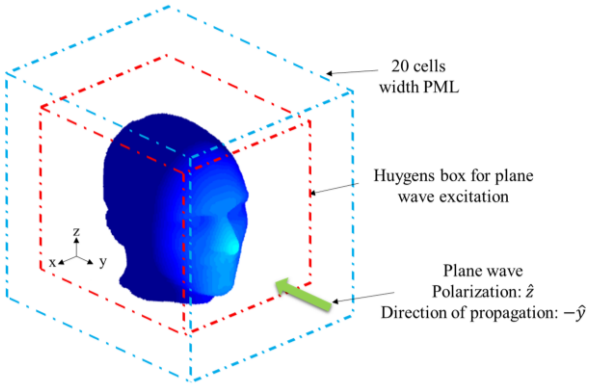

Figure 2: Duke voxel model excited by a plane-wave using Huygens box

The SAR distribution was initially computed at 1 mm resolution, then as a convergence test was conducted by repeating the same simulation with a 0.667 mm mesh-size. As shown in figure 3 below both SAR distributions are in good matching.

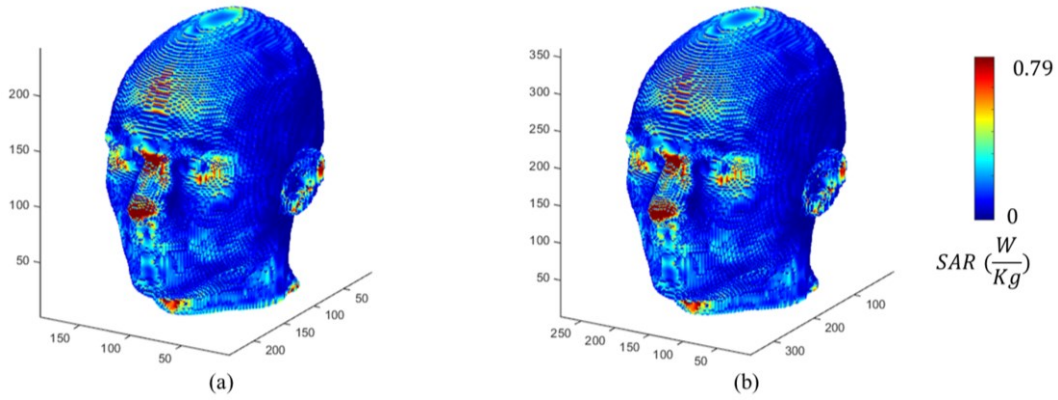

Figure 3: SAR distributions for plane wave excitation at 3.5 GHz, (a) resolution 1 mm, (b) resolution 0.667 mm.

Table 1 below shows the computational expenditures for both simulations shown in figure 3. Where N_c is the number of TLM cells needed to represent the computational domain, N_p is the number of processors used to run the simulator, CPU_t is the corresponding CPU simulation time and N_{it} is the number of iterations used in every simulation. One can observe that, even for the 3.5 GHz which is a relatively small frequency in the 5G band the CPU-time and memory requirements are very high. Repeating the same experiment a higher 5G frequency band

such as, 28 GHz ($\varepsilon_r \approx 16, \sigma \approx 27$ S/m) [5] [7] means a mesh size less than 0.27 mm (1.46 billion cells, and 127 days with 42 processors).

	3.5 GHz	
	1 mm	**0.667 mm**
N_c	36750000	96768000
N_p	37	42
CPU_t	12h45min	37h41min
N_{it}	20000	30000

Table 1: Memory requirements, number of processors and iterations and the corresponding CPU-time (plane wave excitation)

4.2 Duke' head excited by a half-wavelength dipole antenna

In figure 4 below, the Duke head is illuminated by a center-fed half-wavelength dipole antenna. The antenna is made of cupper ($\sigma = 5.96 \times 10^7$ S/m) with a length of 43 mm (43 cells in 1mm resolution and 64 cells in 0.667 mm) and a square cross section of 2 mm side length. An air gap of one cell-size at the center of the antenna is used to place a voltage source with a modulated Gaussian pulse temporal-profile. The antenna is located vertically next to the right-ear with around two cm distance from the skin.

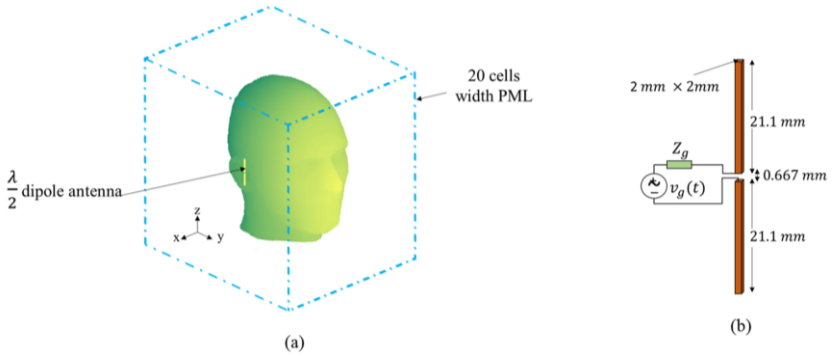

Figure 4: Duke voxel model illuminated by a half-wavelength dipole antenna at 3.5 GHz

Similar to the previous experiment, the SAR distributions were initially simulated at 1 mm resolution, and then were repeated at 0.667 mm resolution to test for convergence. As shown in figure 5 below the SAR distributions for both resolutions are in good matching.

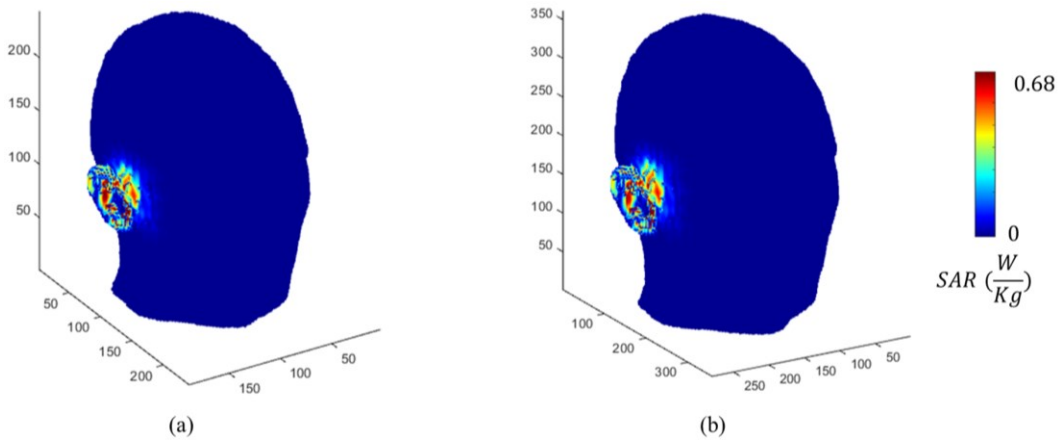

Figure 5: SAR distributions for a half-wavelength dipole antenna at 3.5 GHz, (a) resolution 1 mm, (b) resolution 0.667 mm.

Simulation times and memory requirements are shown in table 2 below, one can observe that the number of iterations is higher than what is used in the previous experiment, even though the same modulated Gaussian pulse temporal profile is used in both experiments. That is due to the high resonance phenomenon in the antenna structure; however, this high number of iterations allows us to compute the input impedance of the antenna.

	3.5 GHz	
	1 mm	**0.667 mm**
N_c	36750000	96768000
N_p	37	72
CPU_t	31h53min	55h04min
N_{it}	50000	75000

Table 2: Memory requirements, number of processors and iterations and the corresponding CPU-time (half-wavelength dipole antenna excitation)

One can observe in Figure 6 the high impact of human head presence in the proximity of the antenna on its input impedance (51.5 Ω difference in input resistance and 13.6 Ω in input reactance). That means the interaction between the head and the antenna modifies the operating setup of the later. Note that to simplify our calculations we used a relatively thick wire antenna (square cross-section of side length of 2 mm, and 43 mm in length). However, if one is interested in using thin wire antennas a very fine resolution should be used to accurately discretize the cylindrical shape of the wire. This can be done by using block meshing approach, with fine meshing applied to the antenna and few cells in its proximity [8].

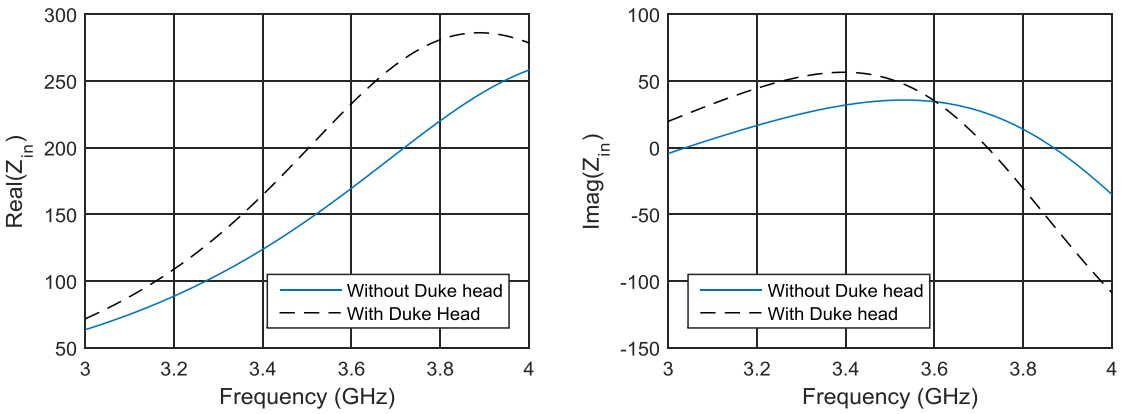

Figure 6: Input impedance of the dipole antenna vs. frequency, impact of Duke' head presence (results are shown for resolution $\Delta x = 0.667mm$)

4.3 Duke' head vs. entire Duke' model excited by a plane wave

In this example, the objective is to study the effect of excluding the rest of Duke' body when computing the SAR in the head. The SAR was computed initially for the entire body as shown in figure 7a (figure 7b is the SAR distribution in the head cut from figure 7a for visualisation purposes). Then, the SAR distribution was computed for the head alone as in the first experiment. In both figure 7a and figure 7c a mesh-size of 2mm was used.

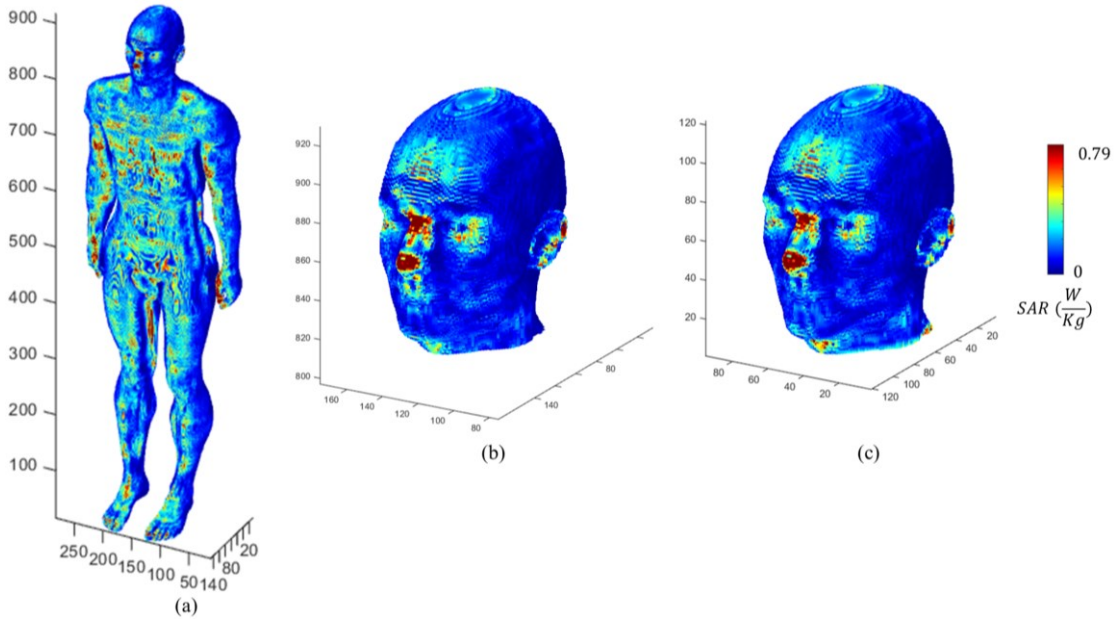

Figure 7: (a) SAR distribution in the entire Duke model illuminated by a plane wave at 3.5 GHz, (b) SAR distribution in the head of figure 7a, (c) SAR distribution in Duke head when head was simulated alone (the rest of the body was excluded from the computational domain)

Similar SAR distributions can be noticed in both figure 7b and figure 7c, with small differences can be observed in the neck region close to the cutting plane of Duke' head (this can be explained by the diffraction/scattering at the artificial discontinuity in the neck in figure 7c). Note that SAR distributions in figure 7b and figure 7c are in good agreement to SAR distributions in figure 3a and figure 3b in the first experiment. From figure 7 one can conclude that at 3.5 GHz the SAR can be computed with a reasonable accuracy in a specific region without the need to include the entire body. In table 3, one can notice big differences in simulation time and the number of TLM cells required to represent the computational domain for both the head alone, and the full Duke model, respectively.

	3.5 GHz (2mm)	
	Head	**Full body**
N_c	4593750	71319500
N_p	62	142
CPU_t	0h25min	7h40min
N_{it}	15000	15000

Table 3: Memory requirements, number of processors and iterations and the corresponding CPU-time (plane-wave excitation Duke' head vs. full Duke' model)

5 Conclusion

A numerical dosimetry procedure-based TD-TLM computational scheme was presented. This method allows for computing the EM-fields in arbitrary complex linear media such as human tissues. This allows for the calculations of SAR (up to 6-10 GHz) or PD (in the millimetric range of the 5G spectrum). Moreover, the possibility to simulate scenarios involving humans and EM-devices permits to evaluate the impact of human presence on their performance. The second objective of this article is to study the effect of considering only a part of the human model (ex. the head) vs. including the full human model in the computation domain. In addition, we study the impact of human tissues presence on the antenna performance in their proximity. Numerical experiments show that a good SAR distribution can be obtained in the head without considering the entire model with a huge memory and CPU-time gain as compared to the case of the entire model. Moreover, the input impedance of the dipole antenna was largely influenced by the presence of Duke head in their near field region.

Acknowledgment

This work benefited from access to CINES computing resources through the 2019-A0060505122 resource allocation attributed by GENCI.

References

[1] Q. Abbasi et al. Advances in body-centric wireless communication: Applications and state-of-the-art. Institution of Engineering and Technology, 2016.

[2] A. R. Guraliuc et al, "Near-Field User Exposure in Forthcoming 5G Scenarios in the 60 GHz Band," in IEEE Transactions on Antennas and Propagation, vol. 65, no. 12, pp. 6606-6615, Dec. 2017.

[3] A. Farhat et al, "TLM Extension to Electromagnetic Field Analysis of Anisotropic and Dispersive Media: A Unified Field Equation." IEEE transactions on microwave theory and techniques 60.8 (2012): 2339-2351.

[4] J. Wlodarczyk, "New multigrid interface for the TLM method." Electronics Letters 32.12 (1996): 1111-1112.

[5] https://itis.swiss/virtual-population/virtual-population/vip2/duke/

[6] A. Ijjeh et al. "Solveur TLM multi-physique pour applications en dosimétrie." 2017.

[7] D. Colombi et al. “RF energy absorption by biological tissues in close proximity to millimeter-wave 5G wireless equipment.” IEEE Access. 2018 Jan 5;6:4974-81.

[8] M. Ney et al. "Block Meshing TLM Based Approach for Low Frequency Antennas Characterization." 2019 International Conference on Electromagnetics in Advanced Applications (ICEAA). IEEE, 2019.